

## Technical Paper

# Fundamental study on dielectric relaxation characteristics of cementitious materials

Tomoko FUKUYAMA \*; Yuki OKAMOTO; Takuya HASEGAWA; and Osamu SENBU

(Received: January 04, 2017; Accepted: May 19, 2017; Published online: July 05, 2017)

**Abstract:** Dielectric frequency response measurement is utilized for a microstructure analyses of materials in various fields. The movements of the positive and the negative charges cause the response, which is so-called dielectric relaxation, and its measurement enables to clarify the interfacial composition of material. For example, the dielectric relaxation analysis of the human body cells is popular in the medical area. Generally speaking, the indices of dielectric relaxation are capacitance, conductance, and susceptance. If the dielectric relaxation measurement is applied to the concrete structure, there is a possibility to perform analyses of the concrete microstructures, because the interfacial compositions of aggregates, cement matrix, or pore solution dominate the dielectric relaxation responses of concrete theoretically. The correlations between concrete properties and dielectric relaxation responses are the significant information of concrete internal microstructures. This paper presents the results of the experimental examinations which were conducted to grasp the influence of the pore solution composition and the electrode interval on the dielectric relaxation properties. As a result, it became apparent that the behaviors of conductive electric charge, electric response charge, and displacement charge explain how sodium chloride and the distance between electrodes affected not only the magnitude of dielectric relaxation properties but also frequency spectrum.

**Keywords:** capacitance, conductance, susceptance, dielectric relaxation, charge behavior.

## 1. Introduction

Dielectric relaxation measurement is widely used as a nondestructive internal inspection method for composite materials in various areas. Charges in materials move according to the frequencies of the electric field applied by an external power supply. The charge movements are the electrical phenomena called polarization. The polarizations form capacitors in each interface of materials. Dielectric and conductive characteristics of the composite material dominate the behaviors of these capacitors in each frequency.

In other words, the dielectric relaxation measurement is an electrochemical technique to clarify internal structure of composite materials by analysis of behaviors of micro capacitors. For example, in the medical area, microstructure analyses of human body cells are carried out by the dielectric relaxa-

tion measurement [1].

In the area of concrete, Koleva [2-4] considered the composite microstructure of hydration products as elements of the electrical circuits. There are three types of electrical paths in a concrete structure, i.e., Continuous Conductive Paths (CCPs), Discontinuous Conductive Paths (DCPs), and Insulator Conductive Paths (ICPs).

Theoretically, current conduction through CCP occurs in the pore solution by ions migration. Therefore, a resistance  $R_{CCP}$  can describe the total impedance of all the CCPs in the mortar statistically. It can be expected for young age concrete or concrete filled with pore solution that  $R_{CCP}$  is inversely proportional to porosity and pore connectivity, whereas  $R_{CCP}$  is positively proportional to the resistivity of the pore solution and the tortuosity (mainly dependent on volume fraction and shape of aggregate grains) of the transport paths (CCPs). It is also related to the geometry of the concrete material (e.g. thickness of the mortar specimen).

Compared with CCP, DCP has more complex impedance expression because of the Discontinuous Points (DPs). The impedance of DCP can be considered consisting of two parts: the continuous portion of DCP and the DP (i.e. cement paste layers).

---

*Corresponding author T. Fukuyama* is an Assistant Professor at Hokkaido University, Sapporo, Hokkaido, Japan.

*Y. Okamoto* is a graduate student at Hokkaido University, Sapporo, Hokkaido, Japan.

*T. Hasegawa* is an Associate Professor at Hokkaido University, Sapporo, Hokkaido, Japan.

*O.Senbu* is a Professor at Hokkaido University, Sapporo, Hokkaido, Japan.

At the DP point, the current has to penetrate through the cement paste layer. However, the cement paste has high resistivity and is usually regarded as an insulator, so a DP is hard to be penetrated through by charges. However, the DP can also be treated as a parallel plate capacitor with the cement paste as its dielectric. Under an alternating electric field, an “apparent electric current” flows to this parallel plate capacitor. We applied dielectric relaxation measurement to cement based materials and confirmed the existence of micro capacitors of cement matrices which Koleva mentioned (Fukuyama [5, 6]). However, little is known about the factors which affect the dielectric relaxation properties of cement-based materials.

The goal of this study is the development of the concrete pore structure analysis method utilizing the dielectric relaxation measurement which clarifies the behavior of electric charges. In this paper, to obtain the fundamental information about the activity of electric charges associated with frequency changes (dielectric relaxation), the empirical examination was performed to examine the influences of the pore solution composition (sodium chloride), the admixtures (blast furnace slag and fly ash), and the electrode interval on the dielectric relaxation properties.

## 2. Dielectric relaxation measurement

### 2.1 Polarization

The knowledge about the polarization of the material is essential to understand the dielectric relaxation measurement. The polarization means the relative position changes of the positive and negative charges which are under an electric field. Also, there is another polarization called the “interface polarization” which is formed at the interface between materials. It takes a certain period to reach an equilibrium of polarization after applying an elec-

tric field. Because this dielectric relaxation characteristic is a feature peculiar to each material, dielectric relaxation data provide much information about electrochemical aspects of the material.

In this paper, the dielectric relaxation indices such as capacitance, conductance, and susceptance were measured to grasp the dielectric relaxation properties of the materials. Outlines about these indices are given in the following sections.

### 2.2 Dielectric relaxation indices

Figure 1 shows a model of a parallel flat plate capacitor [7]. Alternating electric field generates the displacement charge  $QS$  on the electrode surface of the parallel plate capacitor filled with a conductive dielectric material. Any displacement charge  $QS$  does not flow through the dielectric material but goes to the electrode plates alternately via an external circuit. As a result, the movements of these displacement charge  $QS$ s are observed as electric current  $I_C$  from the outside (Eq. (1)). The sensitivity charge  $PS$ s of material are excited by the electric field and move towards the oppositely charged electrode. The behavior of  $PS$  generates an electric field, and it is perceived as capacitance increment of the system by the measurement equipment. The conductive electric charge amount of material determines conductive current  $I_G$ . Moreover, when the conductive electric charge reaches the electrode, it discharges the displacement charge  $QS$  of the electrode, and the external power source provides additional  $QS$ .

As shown in Eq. (2), the summation of  $I_G$  and  $I_C$  is the total current observed in the external circuit. The real part is the conductive characteristic, namely conductance, and the imaginary part of the equation is the electric charge reaction derived from capacitance.

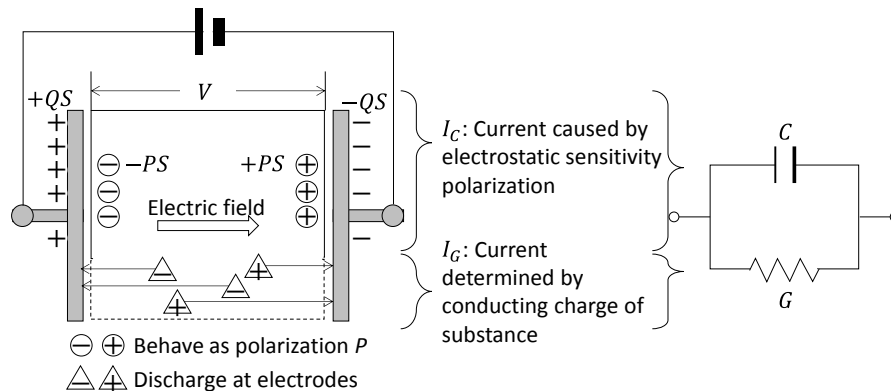


Fig. 1 – Model of parallel flat plate capacitor by Hanai [7]

$$I_C \equiv \frac{dQS}{dt} = \frac{d(CV)}{dt} = C \frac{dV}{dt} = Cj\omega V \quad (1)$$

$$I = I_G + I_C = GV + j\omega CV \quad (2)$$

Where,

$I_C$  is displacement current of parallel plate capacitor, in ampere

$QS$  is displacement charge, in coulomb

$t$  is time, in second

$C$  is capacitance, in farad

$V$  is complex voltage, in volt

$I$  is total current of circuit, in ampere

$I_G$  is conductive current linearly with conductance  $G$ , in ampere

$G$  is conductance, in siemens.

displacement charge  $QS$ , and the imaginary part becomes the contribution to the amount of total electric charge of the conductive electric charge (Eq. (4)).

$$I = \frac{dQS}{dt} = j\omega QS \equiv j\omega(C^*V) = G^*V \quad (3)$$

$$= GV + j\omega CV$$

$$= GV - jBV$$

$$QS = \frac{I}{j\omega} = \frac{G^*V}{j\omega} = C^*V = CV - j\frac{G}{\omega}V \quad (4)$$

Where:

$QS$  is complex total electric charge, in coulomb

$C^*$  is complex capacitance, in farad

$G^*$  is complex conductance, in siemens

$B$  is susceptance, in siemens.

### 3. Materials

Table 1 shows the mix proportion of the cement paste specimens, and the properties of cement, blast furnace slag, and fly ash are given in Table 3 and Table 4, respectively. In this research, the ion concentration difference between each material is one of the experimental factors.

Table 1 – Cement paste mix proportion

Series	IN (%)	W/B (%)	Unit water amount (kg/m <sup>3</sup> )	Unit mass (kg/m <sup>3</sup> )		L (mm), Curing [Name of specimen]
				OPC	BF or FA	
OPC	-	40	175	438	-	30, 3% salt water curing [L30NaCl]
BF	50			219	219	30, tap water curing [L30]
FA	20			350	88	90, tap water curing [L90]

NOTE: IN - internal percentage based on mass of cement; W – water; B - binder; OPC - Ordinary Portland cement (density: 3.16 g/cm<sup>3</sup>); BF - blast furnace slag (density: 2.91 g/cm<sup>3</sup>); FA - fly ash (density: 2.32 g/cm<sup>3</sup>), L - length of cement paste specimen (= distance between electrodes)

Table 2 – Ordinary Portland cement test result

	D (g/cm <sup>3</sup> )	A (cm <sup>2</sup> /g)	MgO (%)	SO <sub>3</sub> (%)	IL (%)	Total alkali (%)	Cl <sup>-</sup> (%)
JIS R 5210	-	2,500 <	< 5.0	< 3.5	< 5.0	< 0.75	< 0.035
Average	3.16	3,340	2.45	2.95	2.35	0.42	0.022
Maximum (Minimum)	-	-	2.50	(1.99)	2.45	0.52	0.024

NOTE: D - density, A - specific surface area, IL - ignition loss

Table 3 – Blast furnace slag test result

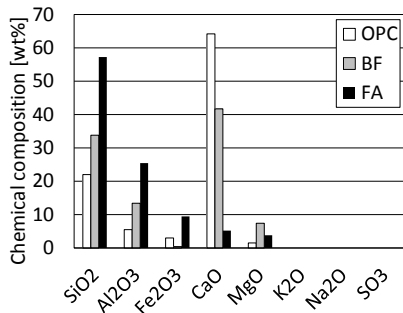
	Density (g/cm <sup>3</sup> )	A (cm <sup>2</sup> /g)	Activity index (%)			RF (%)	MgO (%)	SO <sub>3</sub> (%)	IL (%)	Cl <sup>-</sup> (%)
			7 days	28 days	91 days					
JIS A 6206	2.80 <	3,500 < < 5,000	55 <	75 <	95 <	95 <	< 10.0	< 4.0	< 3.0	< 0.02
Test result	2.91	4,030	73	95	113	102	5.8	0	0.3	0.004

NOTE: gypsum – free; slag basicity 1.84; A - specific surface area; RF - ratio of flow; IL - ignition loss

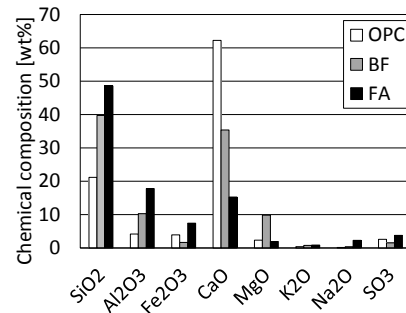
Table 4 – Fly ash test result

	SiO <sub>2</sub> (%)	Moisture (%)	IL (%)	Density (g/cm <sup>3</sup> )	Fineness		RF	Methylene Blue[mg/g]
					P (%)	A (cm <sup>2</sup> /g)		
JIS A 6201 Class 2	45.0 <	< 1.0	< 5.0	1.95 <	< 40	2500 <	95 <	–
Test result	64.2	0.08	1.9	2.32	5	4090	104	0.53

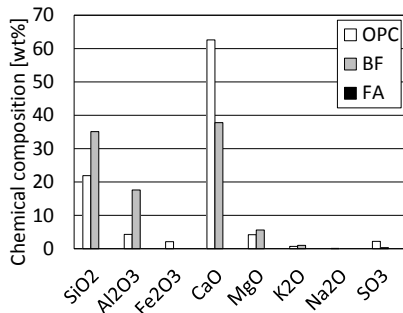
NOTE: IL - ignition loss; P - particle retained on 45 micron sieve; A - specific surface area; RF - ratio of flow [%]



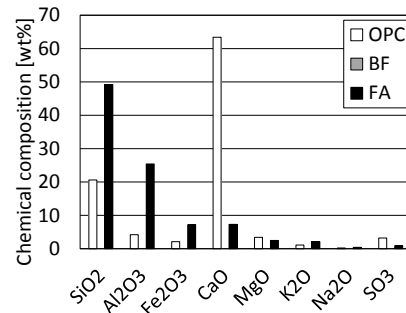
(a) Japan (K<sub>2</sub>O, Na<sub>2</sub>O, SO<sub>3</sub>: NA) [8, 9]



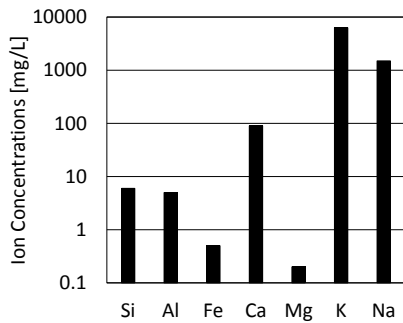
(b) China [10]



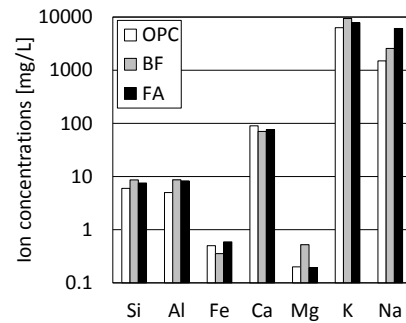
(c) United Kingdom (FA:NA) [11]



(d) Sweden (BF:NA) [12]



(e) Ion concentration of cement specimen pore solution [12]



(f) Rough estimation of ion concentration difference between each specimen [10, 12]

Fig. 2 – Chemical composition example of cement, blast furnace slag and fly ash

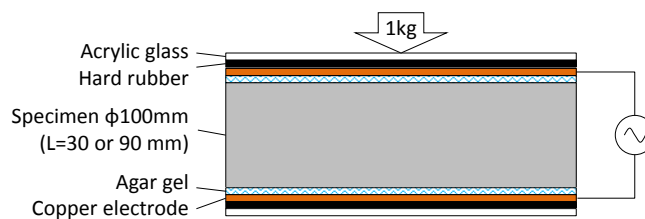


Fig. 3 – Cross section of dielectric measurement configuration

However, pore solution test was not conducted. Hence, ion concentration measurement data of previous researches are utilized as the reference values to estimate the relative relationship of ion concentration between each series.

Figure 2(a)-(d) shows the chemical composition example of cement, blast furnace slag, and fly ash [8-12]. Note that OPC and BF in Fig. 2(a) demonstrate the width values. Hence the averages were taken to describe the graphs. As shown in the figures, the chemical compositions of each material indicate the same tendency in the relative relationship of component ratio. Fig. 2(e) provides the ion concentration information about the cement which is referred in Fig. 2(d). Rough estimations of ion concentration difference between each specimen (Fig. 2(f)) were calculated using the Table 1, Fig. 2(b), (e) and illustrates the effect of materials on the ion concentrations of pore solutions.

Figure 3 illustrates the configuration of dielectric relaxation measurement. Specimens were the  $\phi 100 \times 200$  mm cylinders and were cured in water for two weeks. A wet cutter was used to cut each cylinder into three parts (30, 30, and 90 mm thick). Tap water was used to saturate these specimens under a high vacuum state. However, only for "L30 NaCl", 3% sodium chloride solution was used to saturate these specimens. Generally speaking, the unit of a conductivity of tap water is  $\mu S/cm$ , and the conductivity of the salt water is said to be around 1,000 times of tap water.

The system of electrochemical measurement was composed of two electrodes, and the agar gel was used to reduce the contact resistance between the cement specimen and copper electrode. Furthermore, the copper electrodes were insulated from the external environment by the hard rubber boards and the acrylic glass boards, and the one-kilogram loading made the contact pressure uniform.

The 10mV alternating electric field was applied to the specimen at age 35 days under 20 degrees Celsius and 60% R.H. for dielectric relaxation measurement.

## 4. Results and discussion

### 4.1 Conductivity

Figures 4 and 5 show how the sodium chloride and the specimen length (the distance between electrodes), which varies the electric charges amount between the electrodes, affect conductance of cement paste specimens. Also, Fig. 6 shows the raw data of susceptance. Conductance is an integration of the frequency responses of charges, such as conductive electric charge and electric response charge  $PS$ . Moreover, susceptance represents the quantity

of displacement charge  $QS$  which is supplied from an external power source depending on the behavior of the electric response charge  $PS$ . The mobility of charges, and the quantity of electric response charge  $PS$  and the conductive electric charge differ for each material.

It is a little difficult to compare the absolute value of each specimen's conductance, because of their initial charge condition variance. Whereas the differential value of conductance  $d(\log G)$  or susceptance  $B$  is a combination amount of the electric response charge  $PS$ s, the conductive electric charges, and the displacement charge  $QS$ , which are activated at each frequency. Therefore, the initial charge of the system does not affect these indices. By the above-mentioned reason, the behaviors of each specimen's electric charges are interpreted by Fig. 5 and Fig. 6.

According to Fig. 5(a)-(c), the values of  $d(\log G)$  (quantity of electric charge to contribute to conductance) decrease gradually from  $10^6$  Hz and keep advancing with an approximately constant value in lower frequencies. The  $d(\log G)$  traces begin to decrease again from the  $10^2$  Hz neighbor; and the onset points of the decrease are in order of L30, L30NaCl, L90. Conductance is dominated by the quantity of the electric response charge  $PS$ s and the quantity of conductive electric charges. However, the electric charges do not arrive at the electrodes instantly in higher frequency range, and the delays of charges cause arrival time lag in the lower frequency range. In other words, the result of L90 around  $10^2$  Hz shows the arrival time differences. Due to the above reason, there is no appreciable arrival time difference between L30 and L30NaCl (they have the same length) in Fig. 5.

The contribution to the conductance of the electric response charge  $PS$  is said to decrease in the lower frequency range of Fig. 6. The susceptance of  $10^6$  Hz vicinity shows the change that is the same as the conductance of Fig. 5, and the influence of the electric response charge  $PS$  of this part is obvious. On the other hand, from  $10^2$  Hz to  $10^0$  Hz the susceptance has zero value and does not contribute to the conductance. Hence, the conductance of Fig. 5 at  $10^2$  Hz to  $10^0$  Hz reflects the conductive electric charge contained in the materials. Also, from the distribution of susceptance (reaction amount of electric response charge  $PS$ ), L90 is the largest and L30NaCl is the smallest. Because the electric response charge  $PS$ s mirror the dielectric characteristics of each material, the susceptance of L30NaCl containing sodium chloride which is easily ionized is low, and the susceptance of L90 where there is much electric response charge  $PS$  quantity between the electrodes is high. Also,

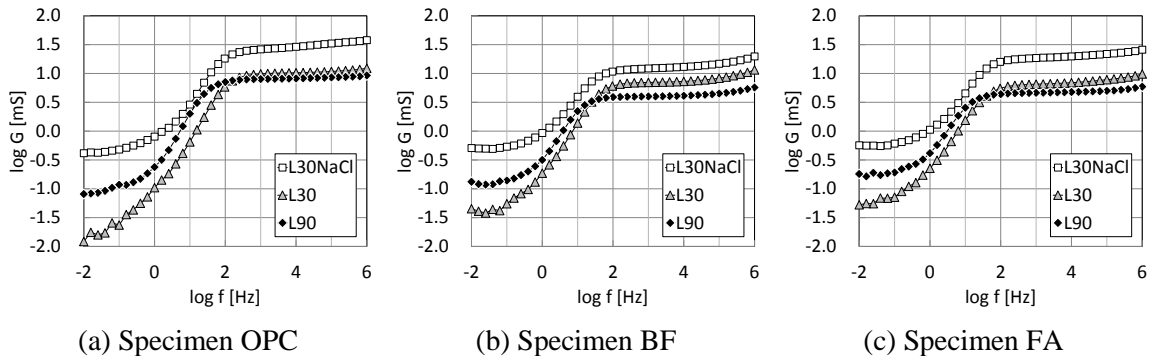


Fig. 4 – Measured value of conductance

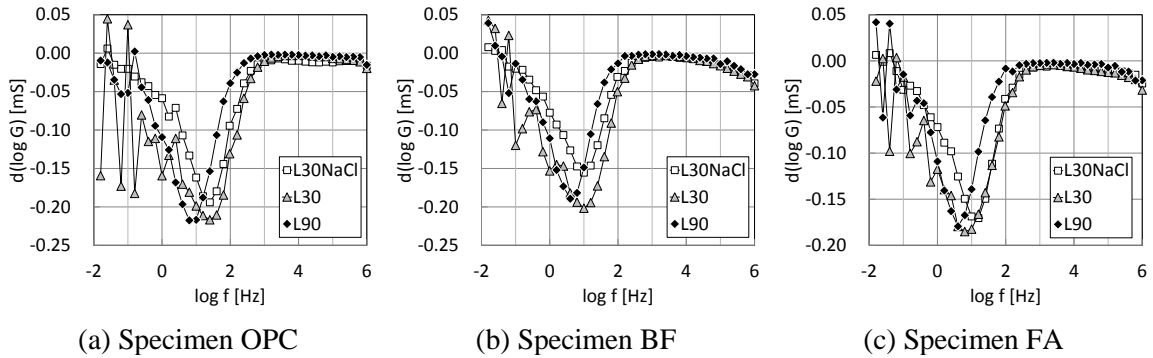


Fig. 5 – Differential value of conductance

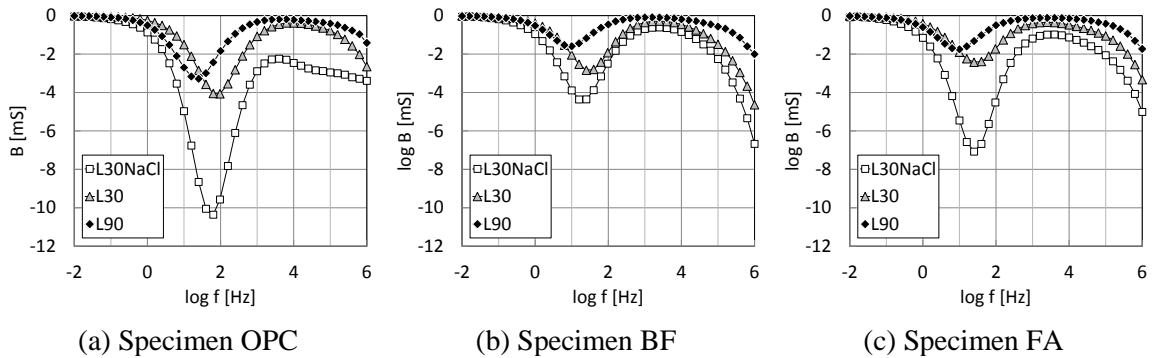


Fig. 6 – Measurement value of susceptance

the peak of the frequency distribution expresses the influence of time lag which results from the distance between the electrodes.

From the result, the  $d(\log G)$  frequency distributions of these three specimens draw the almost same traces under the electric field of 10 mV (the voltage decides the movement speed of the electric charge). However, a content ratio of electric response charge  $PS$  and conductive electric charge differs depending on material composition, and the response lag varies with the material amount ratio. In the lower frequency range, there is enough time for electric response charge  $PS$  to arrive at the measurement electrodes. Therefore, the effects of the electrodes interval appear on the conductance.

Also, the effects of admixtures are the electric charge mobility, which is determined by pore struc-

ture of the cement hydrate, and the chemical composition of pore solution, and appear in susceptance that represents electric response charge  $PS$ .

#### 4.2 Capacity

Figures 7 and 8 show how the sodium chloride and the specimen length (distance between electrodes) affect the capacitance of cement paste specimens. Fig. 7 shows the raw data of capacitance and Fig. 8 shows the differential value of capacitance.

According to Fig. 7(a)-(c) and Fig. 8(a)-(c), the capacitance frequency distributions of each specimen show the same shape change basically. The size of the capacitance is fixed by two following factors. 1) A formed electric field by the electric response charge  $PS$  which arrives at the electrodes.

If the measurement frequency becomes lower, charges have more time to move to the electrodes. This electric field is measured as an increase of capacity and the capacitance of the lower frequency range grows big. 2) The reduction of displacement charge  $QS$  on the electrode. Discharge of displacement charge  $QS$  occurs by conductive electric charges arriving at the electrode.

Both factors reduce electric field formed by displacement charge  $QS$ . According to Fig. 8, the values of  $d(\log C)$  were smallest in the  $10^2$  Hz neighbor. L30NaCl started to increase at the highest frequency and was followed by L90 and L30, in order. It can be realized that the increase in capaci-

tance due to the charges of sodium chloride solution is more obvious than the other specimens.

The influence of admixture was not clear in capacitance. This is because the discharge of displacement charge  $QS$  by the conductive electric charges reduce electric field formed by displacement charge  $QS$ s more efficiently than the formation of the electric field by electric response charge  $PS$ s. In other words, whether the charge is positive or negative is important, but the kind of the ion is not so significant even if admixtures changed the chemical composition of the pore solution.

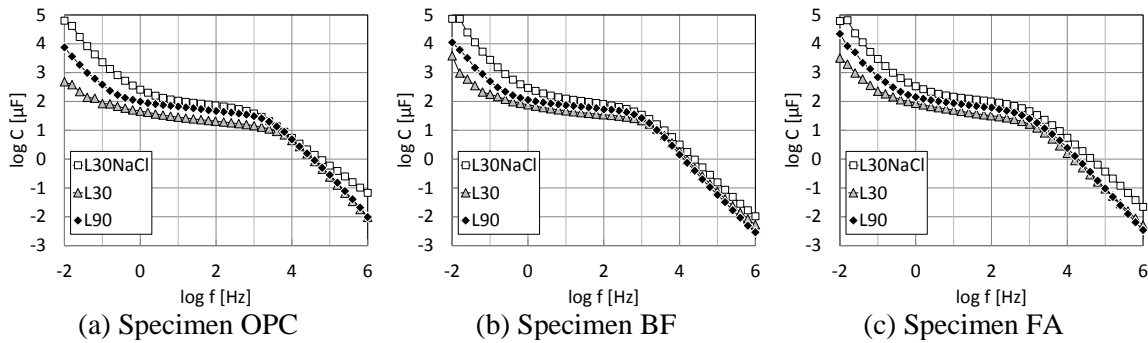


Fig. 7 – Measured value of capacitance of cement paste

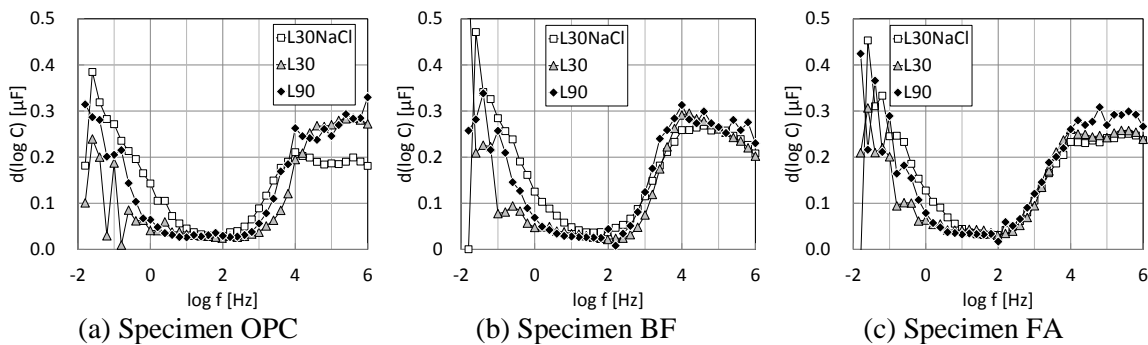


Fig. 8 – Differential value of capacitance

### 5. Conclusions

In this paper, the influences of the sodium chloride solution and the distance between the measurement electrodes on the dielectric relaxation properties were reported. The behaviors of conductive electric charges, electric response charge  $PS$ s, and displacement charge  $QS$ s explain how the sodium chloride and the distance between electrodes affected not only the magnitude of dielectric relaxation properties but also frequency spectrum.

### Acknowledgements

The authors would like to thank Mr. Takayuki Noda and our laboratory members at Hokkaido University for their contribution. The study was financially supported by Grants-in-Aid for scientific

research A (26709038) from Japan Society for the promotion of science, the Asahi Glass Foundation, and Northern Advancement Center for Science & Technology.

Prof. Takuya Hasegawa who made a significant contribution to the research passed away on August 20, 2016. The authors pray from the bottom of our heart that his soul may rest in peace..

### References

1. Takemae, T.; Azuma Y.; and Kosugi Y. (2000) "Electrical Impedance Tomography Applying the Tetrapolar Circuit Method Using Magnetic Field" in Japanese, Japanese Journal of Medical Electronics and Biological Engineering, 38(3), pp. 44-48.

2. Koleva, D. A.; Copurigliu, O.; van Breugel, K., Ye, G.; and de Wit, J. H. W. (2008a) "Electrochemical Resistivity and Microstructural Properties of Concrete Materials in Conditions of Current Flow," *Cement & Concrete Composites*, 30, pp. 731-744.
3. Koleva, D. A.; van Breugel, K.; de Wit, J. H. W.; van Westing, E.; Copurigliu, O.; Veleva, L. P.; and Fraaij, A. L. A. (2008b) "Correlation of Microstructure, Electrical Properties and Electrochemical Phenomena in Reinforced Mortar. Breakdown to multi-phase interface structures. Part I: Microstructural observations and electrical properties," *Materials Characterization*, 59, pp. 290-300.
4. Koleva, D. A.; de Wit, J. H. W.; van Breugel, K.; Veleva, L. P.; van Westing, E.; Copurigliu, O.; and Fraaij, A. L. A. (2008c) "Correlation of Microstructure, Electrical Properties and Electrochemical Phenomena in Reinforced Mortar. Breakdown to multi-phase interface structures. Part II: Pore network, electrical properties and electrochemical response," *Materials Characterization*, 59, pp. 801-815.
5. Fukuyama, T.; Okamoto, Y.; Hasegawa, T.; and Senbu O. (2017) "DIELECTRIC RELAXATION CHARACTERISTICS OF CEMENT PASTE SPECIMENS INFLUENCED BY ADMIXTURE AND PORE STRUCTURES" in Japanese, *Cement Science and Concrete Technology*, 70(1), pp. 201-208.
6. Fukuyama, T.; Okamoto, Y.; Hasegawa, T.; and Senbu O. (2016) "FUNDAMENTAL STUDY ON DIELECTRIC RELAXATION CHARACTERISTICS OF CONCRETE," The 7th International Conference of Asian Concrete Federation, Hanoi, Vietnam.
7. Hanai T. (2000) Heterogeneous structure and dielectric constant (FUKINSHITSU-KOZO to YUDENRITSU), yoshioka syoten, Kyoto, Japan (*in Japanese*).
8. Nippon Slag Association (2008) Environmental Material Steel Slag (KANKYO SHIZAI TEKKO SLAG) in Japanese, Nippon Slag Association, Tokyo, Japan.
9. Nihon Fly ash kyokai (2015) Coal ash handbook (SEKITAN BAI HANDBOOK), Nihon Fly ash kyokai, Tokyo, Japan (*in Japanese*).
10. Peng G. F.; Feng N. Q.; and Song Q. M. (2014) "Influence of Chloride-Ion Adsorption Agent on Chloride Ions in Concrete and Mortar," *Materials*, 7, pp. 3415-3426.
11. Potgietera J. H.; Delporb D. J.; Verrync S.; and Potgieter-Vermaak S. S. (2011) "Chloride-binding Effect of Blast Furnace Slag in Cement Pastes Containing Added Chlorides," *South African Journal of Chemistry*, 63, pp.108-114.
12. Andersson K. E.; Allard B.; Bengtsson M.; Magnusson B. (1989) "Chemical Composition of Cement Pore Solutions," *Cement and Concrete Research*, 19(3), pp. 327-332.